Available online at www.sciencedirect.com

SciVerse ScienceDirect

Ceramics International 39 (2013) 8559–8563

CERAMICS INTERNATIONAL

www.elsevier.com/locate/ceramint

Short communication

Microstructure, mechanical, and thermal properties of in situ-synthesized $(ZrB_2+SiC)/Zr_2[Al(Si)]_4C_5$ composites

D.D. Guo[a], J. Yang[a,*], L. Yu[a], L.M. Pan[a], T. Qiu[a], J.X. Zhang[b]

[a]*College of Materials Science and Engineering, Nanjing University of Technology, Nanjing 210009, China*
[b]*State Key Laboratory of High Performance Ceramics and Superfine Microstructures, Shanghai Institute of Ceramics, Chinese Academy of Sciences, Shanghai 200050, China*

Received 19 February 2013; received in revised form 4 April 2013; accepted 4 April 2013
Available online 11 April 2013

Abstract

Based on thermodynamic analysis, densified 30 vol% $(ZrB_2+SiC)/Zr_2[Al(Si)]_4C_5$ composites were prepared by in situ hot pressing at 1850 °C. The microstructure, mechanical, and thermal properties of the composites were characterized. As reinforcements, ZrB_2 and SiC incorporated by in situ reaction significantly improved the mechanical and thermal properties of $Z_2[Al(Si)]_4C_5$. Compared with monolithic $Z_2[Al(Si)]_4C_5$, the composite showed superior Young's modulus (425 GPa), room temperature flexural strength (621 ± 33 MPa), high-temperature flexural strength (404 ± 13 MPa, 1300 °C, air), fracture toughness (7.85 ± 0.29 MPa m$^{1/2}$), and Vickers hardness (16.7 ± 0.4 GPa). The composite also exhibited a similar heat capacity to but significantly higher thermal conductivity than $Z_2[Al(Si)]_4C_5$.

Keywords: C. Mechanical properties; C. Thermal properties; In situ synthesis; $(ZrB_2+SiC)/Zr_2[Al(Si)]_4C_5$ composites

1. Introduction

$Zr_2[Al(Si)]_4C_5$ is a new quaternary layered carbide formed by adding Al and Si to ZrC. This compound has excellent properties, such as high melting point, retained strength at elevated temperatures, and a relatively good thermal shock resistance [1–5]. Young's modulus of $Zr_2[Al(Si)]_4C_5$ decreases slowly with increasing temperature. $Zr_2[Al(Si)]_4C_5$ can retain 81% of its Young's modulus at various temperatures (from room temperature to 1580 °C). Therefore, $Zr_2[Al(Si)]_4C_5$ is considered as a promising ultra high-temperature material for re-entry and hypersonic vehicles [3–5]. However, the hardness, toughness, and oxidation resistance of $Zr_2[Al(Si)]_4C_5$ remain unsatisfactory [5] compared with other high-temperature structural materials, thereby limiting the application of the material. Incorporating a second phase is known to be an effective method to overcome the aforementioned weaknesses. He et al. [6,7] and Chen et al. [8,9] prepared SiC-reinforced $Zr_2[Al(Si)]_4C_5$ composites that show superior comprehensive performance compared with $Zr_2[Al(Si)]_4C_5$. In recent years, a synergy mechanism between two or more strengthening and toughening phases/methods has been reported. Such mechanism demonstrates considerable enhancement and toughening effect compared with individual toughening phases/methods. In our previous work [10,11], in situ $(TiB_2+TiC)/Ti_3SiC_2$ composites and $(TiB_2+SiC)/Ti_3SiC_2$ composites were prepared by hot-pressing and sintering, respectively. The TiB_2 grains and TiC or SiC grains that were incorporated by in situ reaction improved the comprehensive properties of the Ti_3SiC_2 matrix.

Compared with traditional preparation methods, in situ synthesis shows many advantages in the fabrication of composite ceramics. These advantages include uniform distribution and fine grain size of reinforcements, clean and tightly bonded grain boundary, simplified process, as well as excellent composite properties [12]. Transitional metal borides such as ZrB_2 have high melting point, strength, elastic modulus, and resistance to chemical attack. These compounds can also maintain high strength at elevated temperatures. With the addition of SiC, the ZrB_2–SiC composites show improved strength and fracture toughness as well as superior high temperature oxidation resistance [13–15]. Consequently, ZrB_2–SiC has become the major research subject for ultra high temperature ceramics (UHTCs). Therefore, ZrB_2–SiC can be considered as an ideal binary reinforcement for Zr_2[Al

---

[*] Corresponding author. Tel.: +86 25 83587262; fax: +86 25 83587268.
E-mail address: yangjian1976@163.com (J. Yang).

0272-8842/$ - see front matter © 2013 Elsevier Ltd and Techna Group S.r.l. All rights reserved.
http://dx.doi.org/10.1016/j.ceramint.2013.04.013

(Si)]$_4$C$_5$, with the composites showing great promise as UHTCs. Therefore, based on thermodynamic analysis, novel (ZrB$_2$+SiC)/Zr$_2$[Al(Si)]$_4$C$_5$ composite ceramics were prepared by in situ hot-pressing in the present work, which show optimized microstructure and excellent properties.

2. Experimental

2.1. Materials preparation

Zirconium hydride (99.9%, 0.04 mm), silicon (99.9%, 0.04 mm), aluminum (99.9%, 0.08 mm), graphite (99.9%, 0.08 mm), and B$_4$C powders (99%, 0.35 mm) were used as starting materials. These materials were precisely weighed and mixed for 24 h. The powder mixtures were then put into a graphite mold pre-sprayed with a layer of BN and then preloaded under 3MPa. The compacted mixture was first heated at a rate of 20 °C/min from room temperature to 600 °C and held for 1 h, and then was hot-pressed at 1850 °C for 1 h under the pressure of 25 MPa in Ar atmosphere. For comparison, monolithic Zr$_2$[Al(Si)]$_4$C$_5$ was also prepared following the same process using zirconium hydride, silicon, aluminum, and graphite powders as raw materials.

2.2. Characterization and tests

The bulk density and apparent porosity of (ZrB$_2$+SiC)/Zr$_2$[Al(Si)]$_4$C$_5$ were determined by the Archimedes method. Phase identification was conducted via an X-ray diffractometer with Cu Kα radiation (ARL X'TRA, Switzerland). The microstructure of the polished and fractured surfaces of the samples was observed by scanning electron microscopy (SEM; JEOL, JSM-5900) coupled with energy-dispersive spectroscopy (EDS) for chemical analysis.

The sintered materials were cut, ground, and polished into strips with the size of 3 mm × 4 mm × 40 mm, 2 mm × 4 mm × 20 mm and 1.8 mm × 4 mm × 36 mm for strength, toughness and the elastic moduli tests, respectively. Three-point bending was applied to measure room temperature and high-temperature bending strength using a span of 30 mm with a crossing speed of 0.5 mm/min. The high-temperature flexural strength (1300 °C) in air was tested in a high-temperature universal testing machine. The fracture toughness (K_{IC}) was measured using the single-edge notched beam method with a crosshead speed of 0.05 mm/min. The notch with a depth of 4mm deep and wide was made $\leq$0.28mm. Five samples were used both in strength and toughness measurements. Indentation tests were carried out to determine Vickers hardness at room temperature using a Vickers diamond indenter. The indention were made using a load of 9.8 N with a dwell time of 10 s. Five measurement runs were carried out to determine the average value.

The coefficient of thermal expansion (CTE) was measured using a Setsys-24 thermal mechanical analyzer (Linseis L75 Platinum Series) from 100 °C to 1200 °C with a heating rate of 5 °C/min under flowing Ar. The dimension of the sample for CTE measurement was 20 mm × 3.5 mm × 3.5 mm. The specific heat capacity C_p and thermal diffusivity α (sample size ϕ 12.7 mm × 2 mm) were measured using laser-flash technique from 25 °C to 1200 °C with a heating rate of 20 °C/min under flowing Ar. The thermal conductivity k was calculated according to the following equation:

$$k = \rho C_p \alpha$$

where ρ, C_p, and α are the sample density, specific heat capacity and thermal diffusivity, respectively.

3. Results and discussion

3.1. Thermodynamic analysis

ZrH$_2$ decomposes into Zr and H$_2$ during the heating process. The as-produced Zr then reacts with other raw materials as follows:

$$2Zr + 3.6Al + 0.4Si + 5C \rightarrow Zr_2[Al(Si)]_4C_5, \quad (1)$$

$$2Zr + Si + B_4C \rightarrow 2ZrB_2 + SiC \quad (2)$$

Therefore, the general reaction can be described as follows:

$$5ZrH_2 + 5.3Al + 1.7Si + 7.5C + B_4C \rightarrow 1.5Zr_2[Al(Si)]_4C_5 + 2ZrB_2 + SiC + 5H_2 \quad (3)$$

In the present work, the volume fraction of (ZrB$_2$+SiC) and Zr$_2$[Al(Si)]$_4$C$_5$ in the composites is designed to be 30% and 70%, respectively, according to reaction (3).

3.2. Microstructure

Fig. 1 shows the XRD patterns of the monolithic Zr$_2$[Al(Si)]$_4$C$_5$ and the (ZrB$_2$+SiC)/Zr$_2$[Al(Si)]$_4$C$_5$ composites. Three phases, namely, Zr$_2$[Al(Si)]$_4$C$_5$, ZrB$_2$, and β-SiC and α-SiC (mainly 4 H) are identified in the composites. Zr$_2$[Al(Si)]$_4$C$_5$ is the major crystal phase, indicating the successful preparation of in situ (ZrB$_2$+SiC)/Zr$_2$[Al(Si)]$_4$C$_5$ composites. Fig. 2 shows the backscattered electron image of a polished surface and the EDS analysis results of the composites. The synthesis of (ZrB$_2$+SiC)/Zr$_2$[Al(Si)]$_4$C$_5$ composites is furthermore confirmed by the EDS analysis. As shown in Fig. 2, the average grain size of SiC and ZrB$_2$ is about

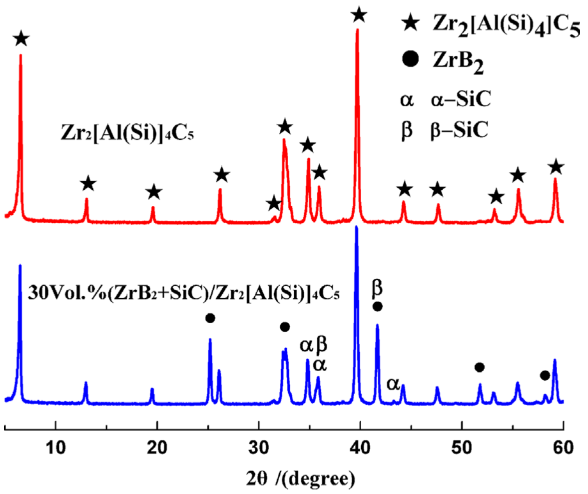

Fig. 1. XRD patterns of as-synthesized (ZrB$_2$+SiC)/Zr$_2$[Al(Si)]$_4$C$_5$ composite and Zr$_2$[Al(Si)]$_4$C$_5$.

0.8 ± 0.5 μm and 1.7 ± 0.8 μm, respectively. The average grain size of $Zr_2[Al(Si)]_4C_5$ is 3.5 ± 1.3 μm, and the aspect ratio of the elongated grains is about 7.3 ± 1.3. Fig. 3(a) and (b) shows the features of the fractured surfaces of the $Zr_2[Al(Si)]_4C_5$ and $(ZrB_2+SiC)/Zr_2[Al(Si)]_4C_5$ composites, respectively. It can be seen that the fractured surface of the $(ZrB_2+SiC)/Zr_2[Al(Si)]_4C_5$ composites is more rough and there are pits and outcrops resulted from grain's pull out. In addition, the $(ZrB_2+SiC)/Zr_2[Al(Si)]_4C_5$ composites exhibit a more densified and fine-grained microstructure than $Zr_2[Al(Si)]_4C_5$. The apparent porosity and bulk density of the $(ZrB_2+SiC)/Zr_2[Al(Si)]_4C_5$ composites are about 0.02% and 4.76 g/cm^3, respectively. The incorporation of ZrB_2 and SiC as reinforcements significantly inhibits the grain growth of the $Zr_2[Al(Si)]_4C_5$ matrix.

3.3. Mechanical properties

Table 1 lists the comparison of some properties of $Zr_2[Al(Si)]_4C_5$, 30 vol% $SiC/Zr_2[Al(Si)]_4C_5$, 20 vol% SiC–ZrB_2, and 30 vol% $(ZrB_2+SiC)/Zr_2[Al(Si)]_4C_5$. Young's modulus of the $(ZrB_2+SiC)/Zr_2[Al(Si)]_4C_5$ composites (425 GPa) is about 17% higher than that of the monolithic $Zr_2[Al(Si)]_4C_5$ ceramic (361 GPa). The flexural strength and fracture toughness of the $(ZrB_2+SiC)/Zr_2[Al(Si)]_4C_5$ composites (621 ± 33 MPa, 7.85 ± 0.29 MPa m$^{1/2}$, respectively) are about twice of those of $Zr_2[Al(Si)]_4C_5$ (353 ± 10 MPa, 3.88 ± 0.12 MPa m$^{1/2}$, respectively). The Vickers hardness of the composites is 16.7 ± 0.4 GPa, which is 43% higher than that of $Zr_2[Al(Si)]_4C_5$ (11.7 GPa). The high-temperature flexural strength at 1300 °C in air is also measured and compared. The flexural strength of the $(ZrB_2+SiC)/Zr_2[Al(Si)]_4C_5$ composites at 1300 °C in air is 404 ± 13 MPa, which is about 65% of that at room temperature and about 50% higher than that of $Zr_2[Al(Si)]_4C_5$ (261 ± 26 MPa) in air at 1300 °C. In brief, the $(ZrB_2+SiC)/Zr_2[Al(Si)]_4C_5$ composites show significantly improved mechanical properties compared with $Zr_2[Al(Si)]_4C_5$. At the same time, the $(ZrB_2+SiC)/Zr_2[Al(Si)]_4C_5$ composites also show comprehensively superior room-temperature mechanical properties compared with SiC-reinforced $Zr_2[Al(Si)]_4C_5$ composites. It should be also noted that $(ZrB_2+SiC)/Zr_2[Al(Si)]_4C_5$ composites have significantly higher fracture toughness but a much lower density than 20 vol% SiC–ZrB_2 ceramics, the most-studied UHTC.

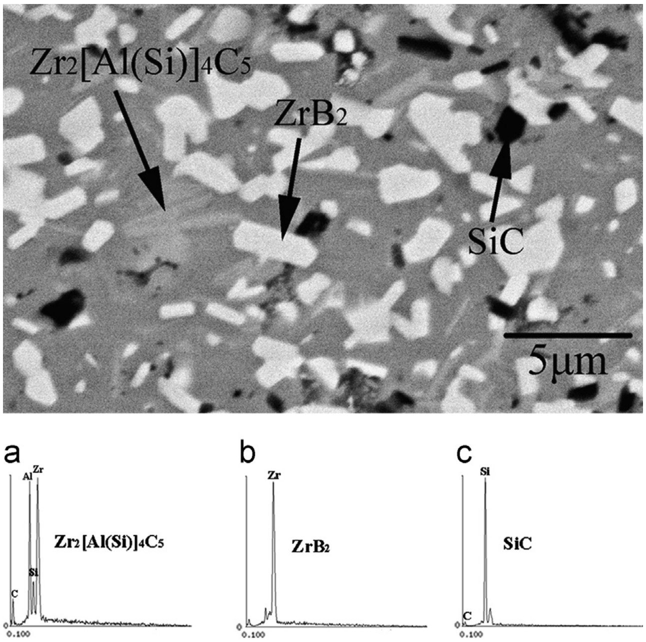

Fig. 2. The backscattered electron image of a polished surface of $(ZrB_2+SiC)/Zr_2[Al(Si)]_4C_5$ composites; EDS analysis of the (a) $Zr_2[Al(Si)]_4C_5$ grains, (b) ZrB_2 grains, and (c) SiC grains.

ZrB_2 and SiC are known to have high hardness (20–30 GPa and 23 GPa, respectively) and stiffness (Young's modulus of 403 GPa and 489 GPa, respectively). Therefore, their incorporation results in higher hardness and stiffness for the composite compared with that for $Zr_2[Al(Si)]_4C_5$. The specific stiffness of the composite is greatly enhanced by adding the two reinforcements with lower density into the $Zr_2[Al(Si)]_4C_5$ matrix. The higher hardness, higher Young's modulus, and mismatched CTE of ZrB_2 and SiC compared with those of the $Zr_2[Al(Si)]_4C_5$ matrix also lead to higher deformation resistance and residual stress toughening. These properties in turn greatly consume fracture energy, resulting in significantly improved strength and toughness. Fig. 3(c) shows the propagation path of the Vickers indentation-induced crack in the $(ZrB_2+SiC)/Zr_2[Al(Si)]_4C_5$ composites. The crack shows deflection and branching during propagation. As mentioned previously, the incorporation of ZrB_2 and SiC induces a grain refinement effect, which significantly improves the strength of the composites.

3.4. Thermophysical properties

The thermal expansion behavior of the composite (373–1473 K) is shown in Fig. 4. The CTE, yielded by the least-

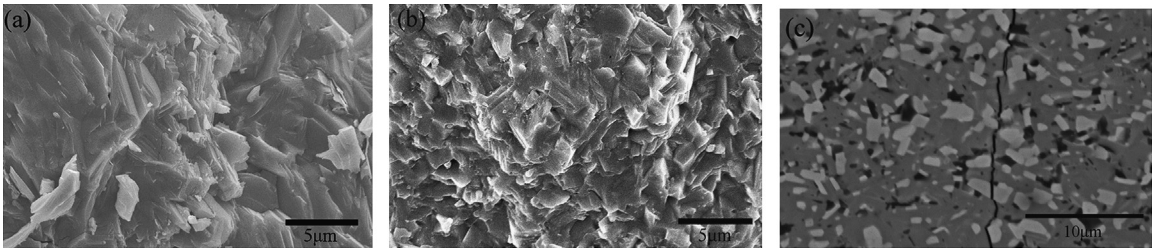

Fig. 3. SEM images of the fractured surface of (a) $Zr_2[Al(Si)]_4C_5$ and (b) $(ZrB_2+SiC)/Zr_2[Al(Si)]_4C_5$. (c) Typical micrograph of the crack propagation on the polished surface of the $(ZrB_2+SiC)/Zr_2[Al(Si)]_4C_5$ composite.

Table 1
Comparison of some properties of $Zr_2[Al(Si)]_4C_5$, 30 vol% $SiC/Zr_2[Al(Si)]_4C_5$ [6], 20 vol% $SiC–ZrB_2$ [14], and 30 vol% $(ZrB_2+SiC)/Zr_2[Al(Si)]_4C_5$.

Properties	$(ZrB_2+SiC)/Zr_2[Al(Si)]_4C_5$	$Zr_2[Al(Si)]_4C_5$	$SiC/Zr_2[Al(Si)]_4C_5$	$ZrB_2–SiC$
Measured density (g cm^{-3})	4.76	4.45	4.01	5.72
Young's modulus (GPa)	425	361 [3]	386	466
Vickers hardness (GPa)	16.7 ± 0.4	11.7 [3]	16.4	24
Bending strength (MPa)	621 ± 33	353 ± 10	353 ± 19	1033 ± 94
Bending strength at 1300 °C (MPa)	404 ± 13	261 ± 26	—	—
Fracture toughness (MPa $m^{1/2}$)	7.85 ± 0.29	3.88 ± 0.16	6.62 ± 0.19	4.4 ± 0.2
Coefficient of thermal expansion ($\times 10^{-6}$ K^{-1})	7.99	8.1 [3]	7.2	—
Specific heat capacity (J kg^{-1} K^{-1})	544.3	567 [3]	584	—
Thermal conductivity(W m^{-1} K^{-1})	22.9	12 [3]	25.3	—

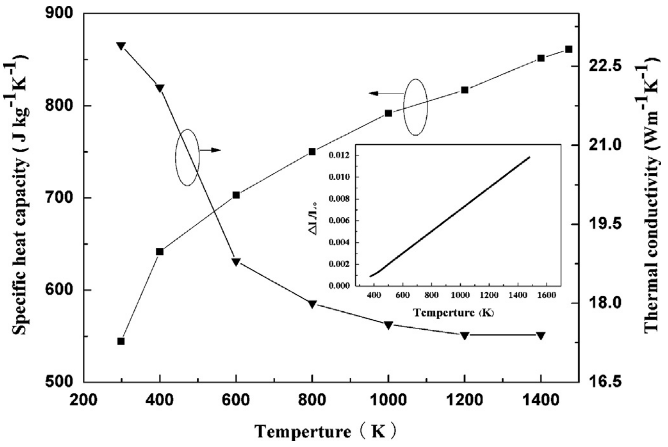

Fig. 4. Temperature dependence of specific heat capacity and thermal conductivity of the $(ZrB_2+SiC)/Zr_2[Al(Si)]_4C_5$ composite (thermal expansion of the composite are implanted).

squares fitting of the data is 7.99×10^{-6} K^{-1}, which is slightly lower than that of $Zr_2[Al(Si)]_4C_5$ (8.1×10^{-6} K^{-1}).

Fig. 4 shows the specific heat capacity and thermal conductivity of the $(ZrB_2+SiC)/Zr_2[Al(Si)]_4C_5$ composites (298–1473 K). The specific heat capacity shows an approximately parabolic increase with increasing temperature and is similar to that of $Zr_2[Al(Si)]_4C_5$ [3] over the entire temperature range. The thermal conductivity of the material decreases gradually with increasing temperature. The thermal conductivities at 298 K and 1473 K are 22.9 W m^{-1} K^{-1} and 17.4 W m^{-1} K^{-1}, respectively. Compared with $Zr_2[Al(Si)]_4C_5$ [3], the $(ZrB_2+SiC)/Zr_2[Al(Si)]_4C_5$ composites show significantly improved thermal conductivity over the entire temperature range, which is favorable to the improvement of thermal shock resistance.

4. Conclusions

Dense $(ZrB_2+SiC)/Zr_2[Al(Si)]_4C_5$ composites, in which $Zr_2[Al(Si)]_4C_5$ and (ZrB_2+SiC) account for 70% and 30% in volume fraction, respectively, were successfully prepared by in situ hot pressing. As reinforcements, ZrB_2 and SiC incorporated by in situ reaction significantly improved the mechanical and thermal properties of the $Z_2[Al(Si)]_4C_5$ matrix. Compared with monolithic $Z_2[Al(Si)]_4C_5$, the composite shows superior Young's modulus (425 GPa), room temperature flexural strength (621 ± 33 MPa), high-temperature flexural strength (404 ± 13 MPa, 1300 °C, air), fracture toughness (7.85 ± 0.29 MPa · $m^{1/2}$), and Vickers hardness (16.7 ± 0.4 GPa). The composite also exhibits a similar heat capacity to but significantly higher thermal conductivity than $Z_2[Al(Si)]_4C_5$.

Acknowledgments

This work was supported by the National Natural Science Foundation of China (No. 50872052), the Natural Science Foundation of Jiangsu Province of China (No. BK2011806), the Opening Project of State Key Laboratory of High Performance Ceramics and Superfine Microstructure (No. SKL201108SIC), the Priority Academic Program Development of Jiangsu Higher Education Institutions, and the Program for Changjiang Scholars and Innovative Research Team in University (PCSIRT), IRT1146.

References

[1] K. Fukuda, M. Hisamura, T. Iwata, N. Tera, K. Sato, Synthesis, crystal structure, and thermoelectric properties of a new carbide $Zr_2[Al_{3.56}Si_{0.44}]C_5$, Journal of Solid State Chemistry 180 (2007) 1809–1815.

[2] Z.J. Lin, L.F. He, J.Y. Wang, M.S. Li, Y.W. Bao, Y.C. Zhou, Atomic-scale microstructures and elastic properties of quaternary Zr–Al–Si–C ceramics, Acta Materialia 56 (2008) 2022–2031.

[3] L.F. He, Y.W. Bao, J.Y. Wang, M.S. Li, Y.C. Zhou, Mechanical and thermophysical properties of Zr–Al–Si–C ceramics, Journal of the American Ceramic Society 92 (2) (2009) 445–451.

[4] L.F. He, X.P. Lu, Y.W. Bao, J.Y. Wang, Y.C. Zhou, High temperature internal friction, stiffness, and strength of Zr–Al(Si)–C ceramics, Scripta Materialia 61 (2009) 60–63.

[5] L.F. He, Y.W. Bao, M.S. Li, J.Y. Wang, Y.C. Zhou, Oxidation of $Zr_2[Al(Si)]_4C_5$ and $Zr_3[Al(Si)]_4C_6$ in air, Journal of Materials Research 23 (2008) 3339–3346.

[6] L.F. He, F.Z. Li, X.P. Lu, Y.W. Bao, Y.C. Zhou, Microstructure, mechanical, thermal, and oxidation properties of a $Zr_2[Al(Si)]_4C_5$–SiC composite prepared by in situ reaction/hot-pressing, Journal of the European Ceramic Society 30 (2010) 2147–2154.

[7] L. Wu, L.F. He, J.X. Chen, X.P. Lu, Y.C. Zhou, Reciprocating friction and wear behavior of $Zr_2[Al(Si)]_4C_5$ and $Zr_2[Al(Si)]_4C_5$–SiC composite against Si_3N_4 ball, Journal of the American Ceramic Society 93 (8) (2010) 2369–2376.

[8] G.Q. Chen, R.B. Zhang, X.H. Zhang, W.B. Han, Microstructure and properties of hot pressed $Zr_2[Al(Si)]_4C_5$/SiC composites, Journal of Alloys and Compounds 481 (1–2) (2009) 877–880.

[9] G.Q. Chen, R.B. Zhang, X.H. Zhang, P. Hu, W.B. Han, Oxidation resistance of $Zr_2[Al(Si)]_4C_5$ based composites at ultra-high-temperature, Scripta Materialia 61 (7) (2009) 697–700.

[10] J. Yang, L.M. Pan, W. Gu, T. Qiu, Microstructure and mechanical properties of in situ synthesized $(TiB_2+TiC)/Ti_3SiC_2$ composites, Ceramics International 38 (1) (2011) 649–655.

[11] K. Song, J. Yang, T. Qiu, In situ synthesis of $(TiB_2+SiC)/Ti_3SiC_2$ composites by hot pressing, Materials Letters 75 (15) (2012) 16–19.

[12] G.J. Zhang, Z.Z. Jin, In-situ synthesis of ceramic composites, Materials Review 10 (2) (1996) 62–65.

[13] G.J. Zhang, Z.Y. Deng, N. Kondo, J.F. Yang, T. Ohji, Reactive hot pressing of ZrB_2+SiC composites, Journal of the American Ceramic Society 83 (9) (2000) 2330–2332.

[14] Adam L. Chamberlain, William G. Fahrenholtz, Gregory E. Hilmas, High-strength zirconium diboride-based ceramics, Journal of the American Ceramic Society 87 (6) (2004) 1170–1172.